Engineering and Characterization of Bacterial Nanocellulose Films as Low Cost and Flexible Sensor Material

Rahul Mangayil[a,*], Satu Rajala[b,c], Arno Pammo[c], Essi Sarlin[d], Jin Luo[a], Ville Santala[a], Matti Karp[a], Sampo Tuukkanen[c]

Author affiliations:

[a] Department of Chemistry and Bioengineering, Tampere University of Technology, P. O. Box 541, FI-33101 Tampere, Finland

[b] Digital Health Laboratory, Nokia Technologies, Karaportti 4, FI-02610 Espoo, Finland.

[c] BioMediTech Institute and Faculty of Biomedical Sciences and Engineering, Tampere University of Technology, P.O. Box 692, FI-33101 Tampere, Finland

[d] Department of Materials Science, Tampere University of Technology, P.O. Box 589, FI-33101 Tampere, Finland

[*] Corresponding authors: rahul.mangayil@tut.fi

Abstract

Some bacterial strains such as *Komagataeibacter xylinus* are able to produce cellulose as an extracellular matrix. In comparison to wood-based cellulose, bacterial cellulose (BC) holds interesting properties such as biodegradability, high purity, water-holding capacity and superior mechanical and structural properties. Aiming towards improvement in BC production titer and tailored alterations to the BC film, we engineered three *K. xylinus* strains to overexpress partial and complete bacterial cellulose synthase

operon that encodes activities for BC production. The changes in cell growth, fermentation profile and BC production titers from the engineered strains were compared with the wild type *K. xylinus*. Although there were no significant differences between the growth of wild type and engineered strains, the engineered *K. xylinus* strains demonstrated faster BC production, generating 2–4-fold higher production titer (the highest observed titer was obtained with *K. xylinus*- bcsABCD strain producing 4.3±0.46 g/L BC in 4 days). The mechanical and structural characteristics of cellulose produced the wild type and engineered *K. xylinus* strains were analyzed with stylus profilometer, in-house built tensile strength measurement system, scanning electron microscopy and X-ray diffractometer. Results from the profilometer indicated that the engineered *K. xylinus* strains produced thicker BC films (wild type, 5.1 µm and engineered *K. xylinus* strains, 6.2 - 10.2 µm). Scanning electron microscope revealed no principal differences in the structure of the different type BC films. The crystallinity index of all films was high (from 88.6 to 97.5 %). All BC films showed significant piezoelectric response (5.0 – 20 pC/N), indicating BC as a promising sensor material.

Keywords: *Komagataeibacter xylinus*, bacterial cellulose, bacterial cellulose synthase operon, genetic engineering, piezoelectric material

1. INTRODUCTION

Cellulose, the most abundant biopolymer on earth, is generally obtained from plant sources. According to the world estimate, over 10^{16} kg of cellulose pulp are produced annually, emphasizing the economic importance of this biopolymer [1]. However, harvesting the cellulose content requires harsh pretreatment steps with high energy input and often results in the generation of lignin derived by-products and/or toxic sulfoxides residues [1,2].

The existence of extracellular cellulose production in bacterial genera such as *Komagataeibacter, Enterobacter, Rhodococcus and Sarcina* has been previously reported [3–5]. It has been speculated that for bacteria, this extracellular polymer provides protection from external physicochemical stresses and the possibility to sustain in aerobic environment [5,6]. Among bacteria, the most efficient cellulose producers found in the genus *Komagataeibacter*, of which the strain *K. xylinus* represents the model organism for studying cellulose biogenesis [1]. The highly ordered bacterial cellulose (BC) is synthesized by bacterial cellulose synthase (bcs) operon consisting of four genes – bcsA, bcsB, bcsC and bcsD. The binding of cyclic di-guanosine monophosphate (c-di-GMP) to the cellulose synthase regulatory subunit (bcsB) commences the cellulose biogenesis. This activates the catalytic subunit (bcsA) to synthesize and polymerize linear β-(1,4) glucan chains from uridine diphosphate glucose (UDP-glucose). The cellulose fibrils are subsequently crystallized and secreted to extracellular matrix by bcsD and bcsC, respectively [2,7]. However, the widespread commercial applicability of BC is largely restricted due to low production titer and yields. To surpass this challenge, both random and rational engineering strategies have been attempted in *Komagataeibacter* species. Hungund & Gupta and Wu et al. have reported improved cellulose production in *K. xylinus* through random mutation (chemical and mechanical) approaches [8,9]. Limited genetic engineering has been attempted in *K. xylinus* by optimizing the carbon flow through the cellulose synthesis pathway and by over-expressing the accessory genes flanking the bcs operon genes [10–12]. Though these

strategies have improved the nanocellulose production, the productivity titers were still low even after a long cultivation period of 7 – 14 days.

In comparison to wood cellulose, BC benefit in high level of purity and crystallinity [2,13]. In terms of biopolymer characteristics, BC has superior structural, mechanical, optical, biodegradable and water holding properties [1]. Due to these characteristics, BC is proposed to have commercial applications in health foods, packaging and biomedical fields [2]. Recent studies propose BC as an excellent biomaterial of choice for electrical and sensor applications [14,15]. Production and utilization of BC as a functional material highly supports the bio-economy through the lower dependency to natural resources and improving the process sustainability.

Piezoelectric materials, that generate charge separation under applied mechanical stress, are widely used in various engineering applications (for example, in sensing and actuation). Conventional piezoelectric elements are bulky ceramic structures that have limited usability in growing application areas such as printed electronics or biomedical applications, where flexibility, transparency and biocompatibility are required. The authors have previously demonstrated the use of existing commercial flexible piezoelectric polymer films, such as polyvinylidene fluoride (PVDF) [16–21] and ferroelectret polymer film [22] for sensor applications. PVDF is promising in this context due to its transparency [18] and compatibility with printed electrodes [19,21]. However, the global push towards a restorative bioeconomy demands in implementing new low cost, sustainable and biodegradable materials for sensor development. Wood biomass, which has been conventionally used as bulk products imparts a significant role in bioeconomy. The piezoelectricity of wood has been known for decades [23,24], but not comprehensively explored until very recently. Studies indicate that the high permanent dipole momentum of cellulose nanocrystals reasons for the excellent piezoelectric property of wood-cellulose [25,26]. The applicability of wood-cellulose as a promising piezoelectric biomaterial has been investigated [20,27–30]. However, wood-based cellulose has

certain limitations, such as multi-step mechanical processing to small dimensional constituents resulting in relatively low tensile strength and low flexibility of cellulose films.

By overexpressing the bcs operon genes in *K. xylinus*, we studied the alterations in productivities as well as structural and piezoelectric characteristics of synthesized cellulose. To achieve this, plasmids with partial and complete bcs operon genes were constructed using Gibson assembly and transformed into *K. xylinus*. The cell growth, substrate utilization, fermentation metabolites and BC production of engineered *K. xylinus* and wild type (WT) were studied. Mechanical and structural characteristics of the produced BC were analyzed and compared. Finally, we demonstrate that BC is an excellent biomaterial with significant piezoelectric sensitivity.

2. EXPERIMENTAL SECTION

2.1. Bacterial strains and cultivations conditions. *Escherichia coli* XL1 (Stratagene, USA) was used as the host for genetic engineering procedures and to maintain plasmid constructs. *E. coli* XL1 cells were grown in low salt Lysogeny Broth (LB, pH 7.0) medium [g L^{-1}: tryptone, 10; yeast extract, 5; sodium chloride, 1] supplemented with glucose (0.4%) and tetracycline (10 mg L^{-1}) at 37 ^{o}C and 300 rpm. *K. xylinus* DSM 2325 (DSMZ, Germany) was grown in buffered Hestrin-Schramm (HS, pH 6.0) medium [g L^{-1}: peptone, 5; yeast extract, 5; di-sodium hydrogen phosphate, 2.7 and citric acid, 1.15) amended with glucose (2%). For pre-cultivation, optical density (OD) measurements and genomic deoxyribonucleic acid (DNA) isolation; the HS medium was supplemented with 0.2% cellulase (*Trichoderma reesei* ATCC 26921, Sigma) and the cells were grown at 30^{o}C and 180 rpm. *K. xylinus* precultivation was conducted in two steps to attain better cell growth. *K. xylinus* from glycerol stocks were inoculated in HS medium (5 ml) and cultivated for 4 days at 30^{o}C and 180 rpm. The pre-grown cells were then transferred to 45 ml cultivation medium and grown for 3 days at similar conditions. These pre-cultivated cells (from 45 ml) were used as the seed inoculum. For BC production experiments, *K. xylinus* cells were grown at 30^{o}C under static conditions for 4 days.

2.2. Plasmid construction. Recombinant *E. coli* and *K. xylinus* strains were constructed by cloning *K. xylinus* bcs operon genes (bcsA, bcsB, bcsC and bcsD) to pBAV1C vector by polymerase chain reaction (PCR) and Gibson assembly. *K. xylinus* genomic DNA isolated using GeneJet Genomic DNA purification kit (Thermo Scientific, USA) was used as the template to amplify the bcs genes. The PCR primers to amplify bcs genes were designed based on the sequence information from *K. xylinus* E25 genome (CP004360.1) (for primer sequences see Table S1 in the Supporting Information). The vector backbone pBAV1C-ara [containing chloramphenicol (Cam) resistance gene, arabinose promoter, and terminator loop] was amplified from the original plasmid (pBAV1C-ara-LuxCDE) [31] with primers pBAV1C_fwd and pBAV1C_rev (Table S1 in the Supporting Information). By employing Gibson assembly (New England BioLabs, USA), three plasmids were constructed (pBAV1C-bcsA, pBAV1C-bcsAB, pBAV1C-bcsABCD) and *E. coli* XL1 cells were transformed with the assembly reaction. The transformants were selected by plating LB-agar containing glucose (0.4%), tetracycline (10 mg L^{-1}) and Cam (25 mg L^{-1}). Transformant validations were conducted by plasmid restriction and PCR analysis. Following the validation, the constructed plasmids were transformed into *K. xylinus* by electroporation.

***2.3. K. xylinus* transformation**. For electrocompetent cell preparation, *K. xylinus* cells (from glycerol stocks) were pre-cultivated as described earlier. The pre-grown cells (initial OD_{600nm} 0.02) were transferred to 100 ml HS medium with similar medium supplements and grown until OD_{600nm} 0.6 (30˚C/180 rpm). The cells were transferred to pre-cooled centrifuge tubes, pelleted at 4000 g (4˚C for 12 minutes) and supernatant was discarded. The bacterial pellet was washed with 40 ml ice-cold 1mM 4-(2-hydroxyethyl)-1-piperazineethanesulfonic acid (HEPES, pH 8.0) solution and centrifuged at similar conditions. The wash step with 1 mM HEPES was repeated twice. Following the HEPES wash, the cell pellets were resuspended in 2 ml ice-cold 15% glycerol. Electrocompetent *K. xylinus* cells were aliquoted in Eppendorf tubes and stored at -80 ˚C until use. The plasmids (pBAV1C-bcsA, pBAV1C-bcsAB, pBAV1C-bcsABCD) were transformed into *K. xylinus* using electroporation. Plasmid DNA (250 – 500 ng) was added to 50 µl *K. xylinus*

electrocompetent cells on ice, mixed well and pipetted to 1 mm width electroporation cuvettes (VWR, USA). Electroporation was conducted by applying 2.5 kV (Micropulser, BioRad, USA). The pulsed cells were immediately resuspended in 1.2 ml of prewarmed HS medium containing glucose (2%) and cellulase (0.2%). Subsequently, the cells were transferred to 5 ml culture tubes and incubated at 30˚C and 180 rpm for 16 hours. The overnight-incubated cells were plated on HS-agar containing glucose (2%), cellulase (0.2%) and Cam (250 mg L^{-1}) and incubated at 30˚C for 5 – 6 days. The transformants were then screened and selected for further experiments.

2.4. BC production. BC production experiments were conducted using WT and engineered *K. xylinus* cells (harboring the empty vector pBAV1C and pBAV1C-bcsA, pBAV1C-bcsAB and pBAV1C-bcsABCD plasmids). Pre-cultivations were prepared as mentioned above and fresh inoculum were inoculated to HS medium (25 ml) with glucose (2%) and Cam (for *K. xylinus* constructs). Arabinose (1%) was supplemented to the growth medium to induce overexpression of bcs operon in engineered *K. xylinus* strains. The *K. xylinus* strains were grown at static conditions for 4 days at 30˚C. Upon confirmation of BC production, glycerol stocks were prepared and was used as the inoculum for the pre-cultivations in subsequent experiments. Cell growth, substrate utilization, liquid metabolites (acetate and gluconate) and BC productions from *K. xylinus* strains (WT, pA, pAB and pABCD) were analyzed for 4 days in both agitated (for cell growth) and static (for BC production) conditions, respectively. For growth curve experiments, the pregrown *K. xylinus* cells (in triplicates, initial OD_{600nm} 0.02) were inoculated to 30 ml HS medium containing glucose (2%), cellulase (0.2%) and ethanol (0.35%, for WT) or Cam (250 mg L^{-1}, for *K. xylinus* constructs) and grown at 30˚C/180 rpm. The experiment included WT *K. xylinus* grown in Cam as control. Culture samples for OD measurements were taken at specific time intervals. Substrate utilization, medium pH, liquid metabolite and BC production profile were studied by inoculating pregrown *K. xylinus* cells (initial OD_{600nm} 0.02) to petri dish containing 25 ml growth medium (2% glucose, and 1% arabinose) and ethanol (for WT *K. xylinus*)

or Cam (for *K. xylinus* constructs) in triplicates. The cultures were grown statically for 4 days at 30˚C and culture samples were analyzed individually at specific time intervals.

2.5. BC film preparation and dry weight measurements. To inactivate the attached cells, the BC sheets were collected, rinsed with ultrapure water (Milli-Q, EMD Millipore, Germany) and incubated overnight in 0.5 M NaOH solution at 60˚C. The alkali solution was removed by repeated washing (with ultrapure water) until neutral pH was attained. To remove the medium entrapped within cellulose sheets, the BC was incubated overnight in water at 60˚C. Following the wash steps, the BC was placed in a pre-weighed fresh petri dish, dried at 60 ˚C for 16 hours and the dry weights were measured at room temperature.

2.6. Analytical techniques. *K. xylinus* biomass was determined by measuring the OD_{600nm} using a spectrophotometer (Ultraspec 500pro, Amersham Biosciences, UK). Glucose utilization and end metabolite production were analyzed using High Performance Liquid Chromatography (HPLC) equipped with Shodex SUGAR column (300 mm × 8 mm, Phenomenex), autosamples (SIL-20AC HT, Shimadzu), refractive index detector (RID-10A, Shimadzu) and 0.01M H_2SO_4 as the mobile phase. The HPLC was conducted as described elsewhere [32]. Briefly, one milliliter of culture samples (in triplicates) were centrifuged at 7600 *g* for 10 minutes and the filtered supernatant (0.2 µm filter) was used for HPLC analysis.

2.7. BC film characterization. Thickness measurements were conducted using three pieces (triplicates) of BC film produced from WT and engineered *K. xylinus* strains. The BC pieces were hydrated and placed on a microscopy glass slide to dry under ambient conditions. BC film thicknesses and topographies were measured with a stylus profilometer (Dektak XT, Bruker, USA). Line scans overlapping the glass-BC step were captured from three different locations from each sample. This resulted in nine captured topography curved for each BC synthesized by *K. xylinus* strains used in this study.

Tensile stress tests were performed with an in-house built tensile strength measurement system (micro-robotic FIBRobot; Figure S1 in the Supporting Information). The experimental setup is described in detail elsewhere (Manuscript: Mathias von Essen, Satu Rajala, Jukka Lekkala, and Pasi Kallio, "*A microrobotic method for measurement of piezoelectric transverse d32 and d33 coefficients*", Submitted to Measurement Science and Technology). Briefly, the device includes an imaging setup with a two-axis translation stage (to position the sample in the camera's field of view) and a tensile test module. The latter works by suspending a sample between two clamps and moving the other with a single-axis translation stage, thus creating tension. A strip cut from BC film was placed between two clamps and stretched at a speed of 0.1 mm/s until the breaking point. The system had a force sensor of 20 N and it recorded the force at a sample frequency of 2000 Hz. In a case where the strip ripped inside the clamp or due to tear on its edge, the result was discarded. Data was processed and analyzed with Matlab software.

The surfaces and cross-sections of BC films produced from each *K. xylinus* strains were studied (in triplicates) with scanning electron microscope (SEM; Zeiss ULTRAPlus, Germany). Cross-sectional images were obtained through cryofracture of BC film under liquid nitrogen and by gluing the film to holders containing conductive carbon cement. The samples were coated with a thin carbon layer to provide electrical conductivity prior to SEM imaging.

The crystallinity indices (CI) of BC films was determined with X-ray diffractometer (XRD; Empyrean multipurpose diffractometer, PANalytical B.V, US) with Cu Kα radiation (λ = 1.5405 Å) and 45 kV and 40 mA cathode voltage and current, respectively. The samples were scanned in 2θ between 10° and 40° with step size 0.01 deg/min and step duration 29 s/step. The CI of BC films was determined from the XRD curves using peak deconvolution method [33].

2.8. Piezoelectric sensitivity measurements. Electrode patterns for the piezoelectric sensor measurements were prepared by evaporating 100 nm of silver on a polyethylene terephthalate (PET) substrate through a laser-cut metallic stencil mask. A piece of hydrated BC film, slightly larger than the

round shape electrodes, was sandwiched between two silver electrodes (Figure S2A in the Supporting Information). While dried, the sensor construct was self-standing and BC film was firmly attached to electrodes on both sides. The piezoelectric sensitivity measurement setup has been previously used in the evaluation of the sensor sensitivity of piezoelectric polymer films [16,29] and cellulose nanofibril (CNF) film [20]. The sensitivity measurement setup is schematically presented in Figure S2B in the Supporting Information. Briefly, the piezoelectric sensitivity measurements were conducted by generating a dynamic excitation force using a Mini-Shaker Type 4810 (Brüel & Kjær, Denmark). A commercial high sensitivity dynamic force sensor (model 209C02, PCB Piezotronics, US) was used as a reference sensor for the dynamic excitation force. A load cell (model ELFS-T3E-20L, Measurement Specialties Inc., US) was used as a reference sensor to measure the static force between the sample and shaker's piston. A pretension, producing the static force, was needed to keep the sample in place and prevent the piston jumping off the surface during the measurement. The static force and sinusoidal dynamic excitation force used for measurements were 3 N and 1.4 N with constant frequency of 2 Hz, respectively. The piezoelectric sensitivity values in pC/N were calculated by dividing the amplitude of generated charge signal by the amplitude of applied dynamic force signal. The value of generated charge was measured with a custom-made setup containing a charge amplifier and a 16-bit AD-converter. Sinusoidal amplitude values were solved by fitting sinusoidals to the charge and force signals, as described in the IEEE Standard for Digitizing Waveform Recorders (IEEE Standard 1241). Sensitivities were measured from five different excitation position on the electrode (Figure S2C in the Supporting Information). The same positions were excited from both sides of the sensor, resulting in ten excitations per sensor. The measured sensitivity in the longitudinal direction is closely related to the piezoelectric d_{33} coefficient that describes the electric polarization generated in the same direction as the stress applied [34]. The sensor linearity was measured by increasing the shaking force gradually in steps and monitoring the sensor charge output simultaneously. Commercial poled 28 µm thick PVDF (Measurement Specialties Inc., USA) with known

piezoelectric properties was used as a reference sensors material. Sensor durability measurements were performed using similar experimental setup as described above and sensor shaking period of 1 hour.

2. RESULTS AND DISCUSSION

3.1. Cloning and over-expression of bcs genes in *K. xylinus.* To overexpress the bcs genes in *K. xylinus*, the cellulose synthase genes were PCR-amplified (see primer sequences in Table S1 in the Supporting Information), assembled in pBAV1C vector backbone under the control of arabinose promoter by Gibson assembly and transformed into *E. coli* XL1. Following the validation (Figure S3 in the Supporting Information), the plasmids were transformed by electroporation into *K. xylinus* cells. In spite of several attempts, we were not able to isolate the plasmids from the transformed *K. xylinus* cells. However, clear phenotypic differences were detected in the growth curve and BC production experiments as described below.

Engineered *K. xylinus* harboring the constructed plasmids, pBAV1C-bcsA, pBAV1C-bcsAB and pBAV1C-bcsABCD, will be referred as pA, pAB and pABCD, respectively, in the following text. Differences in pellicle morphologies between BC produced from *K. xylinus* strains could be observed after the incubation period (Figure 1). Except for pABCD, thin cellulose strands were loosely attached to the pellicle produced from other *K. xylinus* strains.

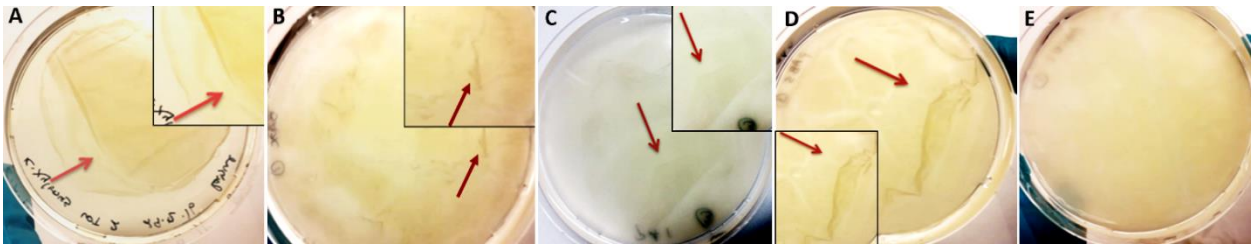

Figure 1. *Morphologies of untreated BC pellicles produced by WT and engineered K. xylinus strains in cultivation plates. (A) WT K. xylinus, (B) WT K. xylinus with ethanol supplementation, (C) pA, (D) pAB and*

(E) pABCD. The inset pictures (indicated with red arrows) show the thin cellulose strands loosely attached to the pellicle.

In the studied conditions, the tested *K. xylinus* strains showed a similar growth profile with differences in BC production (Figure S4 in the Supporting Information). Figure 2 demonstrates the dry weight measurements of BC synthesized by WT and *K. xylinus* constructs. For WT cells, the pellicle formation was incomplete after 4 days of static incubation at 30˚C, resulting in a titer of 0.4 ± 0.0 g/L. A direct correlation between pellicle formation and incubation time has been described previously. Krystynowicz et al. reported a 1.1-fold increase in BC production when the incubation time was increased from 7 to 14 days [35]. Similarly, Kuo et al. reported visible BC production from WT *K. xylinus* grown in HS-glucose medium at day 4 and thereby increasing and reaching saturation at day 12 [36]. Thus low BC production in this study can be associated with short incubation time. However, *K. xylinus*-pBAV1C grown in HS growth medium containing Cam (final ethanol concentration, 0.35%) produced 2.1 ± 0.23 g/L cellulose. Positive effects on cell growth and BC synthesis from ethanol supplementation has been previously reported [37]. In comparison with WT, *K. xylinus*-pBAV1C produced a 4-fold increase in BC production after 4 incubation days. Improved BC production was observed for *K. xylinus* constructs, with pABCD being the best producer synthesizing 4.3±0.46 g/L of cellulose pellicle in 4 days.

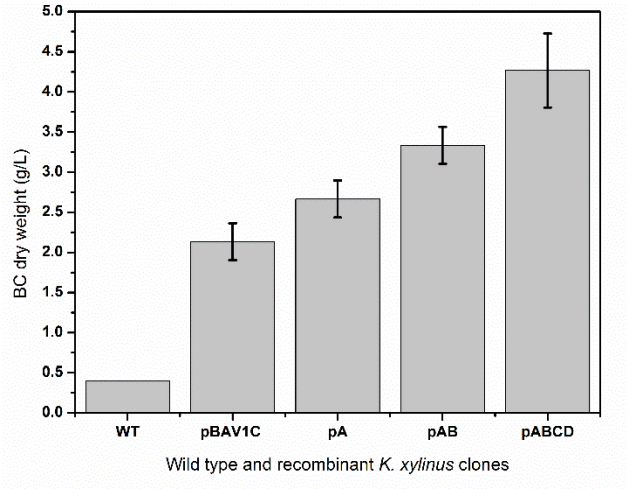

Figure 2*. BC production from wild type (WT) and engineered K. xylinus strains (pA, pAB and pABCD) incubated at static conditions for 4 days at 30˚C. The graph presents mean data and standard deviations (error bars) from triplicate cultivations.*

3.2. BC production, substrate utilization and liquid metabolite production profile. BC production, substrate utilization and liquid metabolite generation from individual *K. xylinus* strains was studied under stationary growth conditions for 4 days at 30^{o}C. For WT and *K. xylinus* constructs, measurable BC was observed from day 2. From Figure 3A it is to be noted that the engineered strains initiated BC production faster than the WT. On comparison with the WT (0.27 g L^{-1}), after 2 cultivation days, 1.5 to 4-fold improved cellulose production was observed from *K. xylinus* constructs (pA, 0.27 g L^{-1}; pAB, 0.93 g L^{-1}; pABCD, 1.07 g L^{-1}). Similar trend in BC production was observed until day 4, generating 1.6 g L^{-1}, 2.13 g L^{-1}, 2 g L^{-1} and 2.93 g L^{-1} of cellulose from WT, pA, pAB and pABCD, respectively. Comparing cellulose production from engineered strains, the BC dry weights from pA and pAB were similar. The bcs operon genes involve in two intermediary steps during the BC formation: (1) formation of beta-1,4-glucan chains from UDP-glucose by c-di-GMP activated bcsA and bcsB and (2) assembly and crystallization of cellulose chains by bcsC and bcsD. Thus, the synthetic bcs operon in *K. xylinus* may contribute in better binding to the cellulose precursor (c-di-GMP) and substrate (UDP-glucose) resulting in faster and improved BC production [38]. Furthermore, this also reasons to our observations that overexpression of bcsA alone will not contribute to an increase in cellulose production. Although the mechanism of bcs machinery is not completely understood, Brown and Saxena (2000) have postulated several models demonstrating the diversity in glycosylation reactions in cellulose biosynthesis, indicating the assembly and crystallization of cellulose chains is as the potential rate-limiting step in BC biogenesis [38]. Coupling the current understanding about BC mechanism with our observations of cellulose production from pABCD, the overexpression of bcsC and bcsD genes can increase BC production.

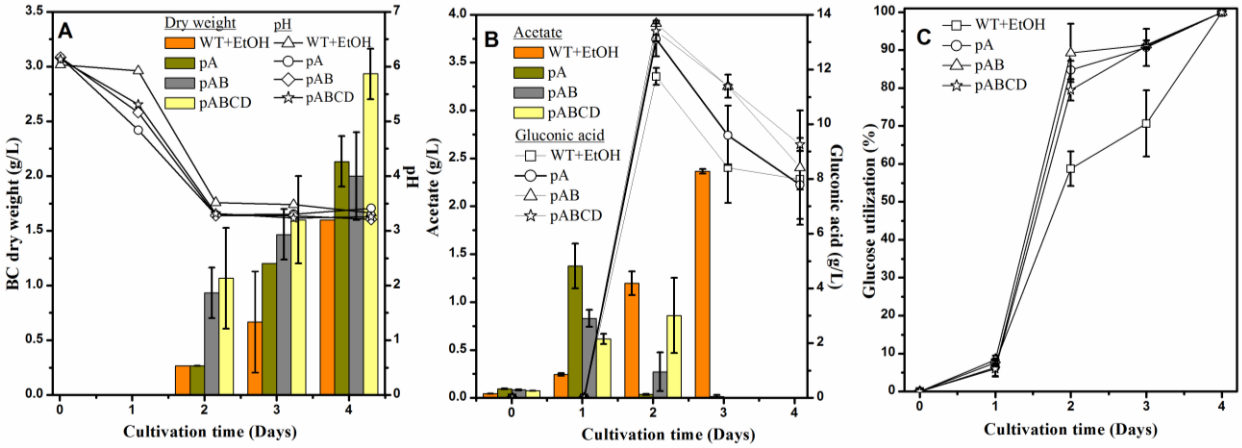

***Figure 3**. BC production, substrate utilization and liquid metabolite production profiles. (A) BC production and the drop in medium pH, (B) end-liquid metabolites and (C) substrate utilization profiles of statically cultivated WT (with ethanol supplementation) and engineered K. xylinus strains. The data points in the above graphs represent the mean experimental result and standard deviations from triplicate cultivations. In some cases, the error bars are smaller than the symbol.*

After 4 days of cultivation, the tested *K. xylinus* strains showed a similar drop in the medium pH (3.3 – 3.5; Figure 3A). This pH drop is associated with the alternative glucose oxidation pathway in *K. xylinus*. In addition to BC biogenesis, *K. xylinus* adopts an alternative glucose oxidation route producing gluconic acid by the catalytic activity of glucose dehydrogenase. This extracellular production of gluconic acid negatively affects the BC production by reducing the glucose availability for cellulose biosynthesis and restricting the bacterial growth (low medium pH). Previous studies have reported that constructing a glucose dehydrogenase (gdh) deficient *K. xylinus* strain enables for better control of medium pH and improved BC synthesis [11,39]. Kawano et al. investigated the fate of gluconic acid in *K. xylinus*. The authors report that the generated gluconic acid can be either converted to keto-gluconate extracellularly for adenosine triphosphate (ATP) generation or transported intracellularly to participate in BC synthesis via the Entner-Doudoroff and pentose phosphate pathways [40]. Similarly, we observed high gluconic acid production from all *K. xylinus* strains tested (Figure 3B). A steep increase in gluconic acid production was observed at day

two (WT, 11.7 g L^{-1}; pA, 13.1 g L^{-1}; pAB, 13.7 g L^{-1}; pABCD, 13.4 g L^{-1}), followed by a gradual decrease with subsequent cultivation days. After four days; HPLC analysis of WT, pA, pAB and pABCD cultivation samples indicated the presence of 8 g L^{-1}, 7.8 g L^{-1}, 8.4 g L^{-1} and 9.3 g L^{-1} of gluconic acid, respectively. In addition to gluconic acid, the presence of acetate was evident in all cultivations. Under the studied conditions, the engineered strains metabolized acetate and glucose better than the WT *K. xylinus* (Figure 3B and 3C). After three days of cultivation, the engineered *K. xylinus* strains metabolized 90% of the glucose, whereas only 70% of the substrate was utilized by the WT. BC biosynthesis in *K. xylinus* is associated with glucose oxidation and consumes as much as 10% of energy derived from catabolic reactions [41]. ATP linked enzymatic pathways in BC biogenesis includes, (a) phosphorylation of glucose to glucose 6-phosphate by glucokinase, (b) conversion of glucose 6-phosphate to glucose 1-phosphate by phosphoglucomutase and (c) UDP-glucose pyrophosphorylase catalyzed UDP-glucose formation from glucose 1-phosphate [42]. Generally, glycolysis in *K. xylinus* generates 2 moles of ATP from 1 mole of glucose, used for both cell biomass and BC synthesis [43]. Acetate oxidation via tricarboxylic acid cycle favors in additional energy generation for biomass generation rather towards BC biosynthesis [43,44]. Thus, effective acetate oxidation can be the reason for faster BC production from engineered *K. xylinus* strains.

3.3. Characterization of BC films. SEM images indicated no remarkable differences between the tested BC films (Figure 4). The cross-sectional view of the films reveals that a layered fiber was more distinguished on the top surface of the films when compared with the bottom surface structure. The BC film thicknesses obtained from the profilometer measurements are provided in Table 1. Average thickness and standard deviation for each film type were obtained from three measured samples per strain type (Table S2 in the Supporting Information). *K. xylinus* construct harboring the complete bcs operon (pABCD) produced the thickest films, followed by pA and pAB. Wild strain *K. xylinus* produced the thinnest films, also the highest deviation in the results.

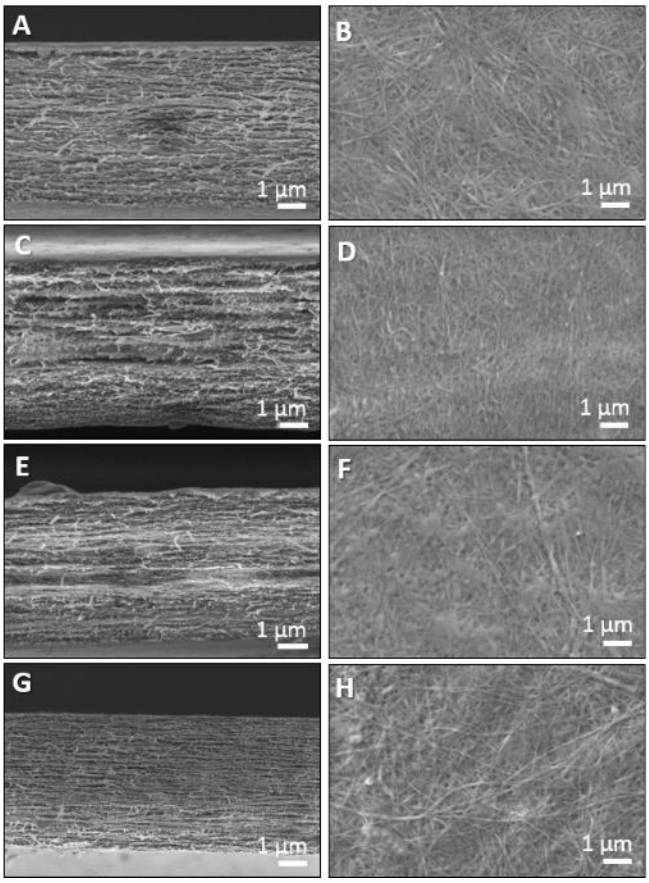

Figure 4. *SEM cross-section (A, C, E and G) and surface views (B, D, F and H) of BC films produced from WT (A and B), pA (C and D), pAB (E and F), and pABCD (G and H).*

Table 1. *Results (mean ± standard deviation) from characterization of BC films produced from WT and recombinant K. xylinus strains.*

BC film produced from the tested *K. xylinus* strains	**Film thickness (µm)**	**Crystallinity index (%)**	**Stress-at-break (MPa)**
WT	4.8 ± 0.8	92 ± 4	47.9
pA	7.4 ± 0.3	97 ± 10	40.7
pAB	6.2 ± 0.3	91 ± 6	80.9
pABCD	10.3 ± 0.6	89 ± 3	48.5

In addition to thickness, profilometer also provided information about the surface topography. All BC film samples had similar topography, which correlates with the SEM studies. The topography curves of dried BC films from different strains are presented in Figure S5 in the Supporting Information. It can be concluded that, in comparison to WT *K. xylinus,* the engineered strains were significantly thicker (2-fold higher thickness for BC films generated by pABCD). In the BC film elongation experiments it was found that the BC from pAB withstood the highest tensile stress of 80 MPa (Figure S6A in the Supporting Information). Some of the curves had sudden, small drops in their force-displacement curves. This was due to creases in the film, which were straighten out when the stretching force increased. The stress at break values in Table 1, were calculated from the measured curves. The values were similar to those reported in related literature [36,45–48].

The BC film XRD spectra shown in Figure 5 displayed peaks of 2θ at 14.6°, 16.9° and 22.7°, which is a characteristic diffraction profile of cellulose I in BC films when produced under static conditions (Here the new reference: Feng, X.; Ullah, N.; Wang, X.; Sun, X.; Li, C.; Bai, Y.; Chen, L.; Li, Z. Characterization of Bacterial Cellulose by Gluconacetobacter Hansenii CGMCC 3917. J. Food Sci. 2015, 80 (10), E2217–E2227). The crystallinity indices (CI) calculated from the diffractogram using the Segal's equation are presented in the Table 1. Average CI and an error as standard deviation are calculated from three measured XRD-curves for each BC film type. Crystallinity of the tested BC films ranged from 88.6 to 97.5 %. Kuo et al. calculated CI of 78 % and 81 % for BC from *K. xylinus* that were cultivated in commercial medium and acetate buffered medium, respectively [36]. Their calculations were made from the XRD patterns alone. Jozala et al. observed crystallinity ranging from 64.6 to 100 %. However, the calculation method was not presented in detail [48]. Cavka et al. calculated CI from XRD spectra of freeze-dried BC using a simple empirical method of Segal et al [49], which is not as accurate as the peak deconvolution method used in this work. Their result for BC produced from *K. xylinus* grown in glucose based medium was 78 %.

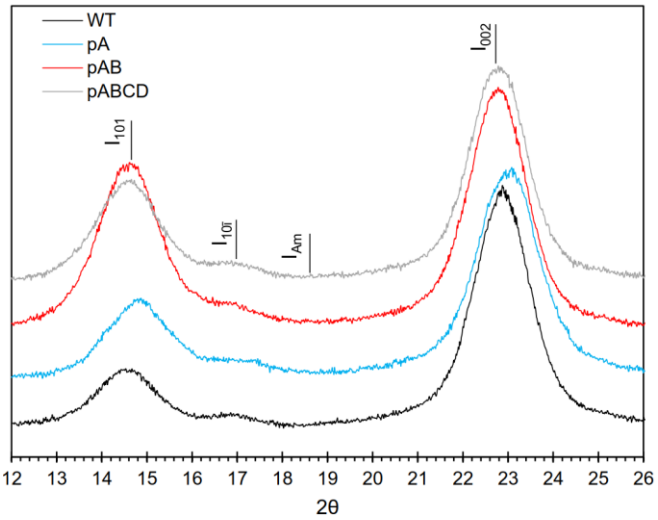

Figure 5. XRD spectra for crystallinity analysis of BC films produced by WT and engineered *K. xylinus* strains.

3.4. Piezoelectric sensitivities of BC films. Piezoelectric sensitivities for assembled piezoelectric BC sensor elements are presented in Figure 6. Piezoelectric sensitivities from 5 to 20 pC/N were obtained here, depending on the bacterial strain used for BC film growth. Wild strain gave the highest piezoelectric sensitivity, close to 20 pC/N, whereas pAB yielded the lowest sensitivity values close to 5 pC/N. Averaged piezoelectric sensitivities for BC film produced by WT, pA, pAB and pABCD were 16.8, 7.3, 5.0 and 8.2 pC/N, respectively.

To examine the piezoelectric properties of BC films, one sensor was further subjected to durability and linearity measurements. The durability of the BC film was tested by measuring the sensor's output charge when exposed to sinusoidal (2 Hz) load cycles for 1 hour with a normal force of 1.4 N. In Figure 7, the output values presented as median amplitudes of 1 min data sections indicate ~96% charge durability over the tested period, demonstrating stable piezoelectric response for the BC film sensor. The piezoelectric response of BC film was further studied by introducing a linearly increasing force load to the BC and PVDF sensors (fabricated using similar sandwiched PET-Cu electrodes as contacts). Similar measurement using a compressive increasing load has been done by Mahadeva et al. [Mahadeva 2016-

paper]. As shown in Figure 8, the sensor charge of both BC and PVDF sensors increase as a function of increasing applied force (1.4 N, 2.7 N, 3.6 N and 4.4 N), suggesting similar piezoelectric behavior in both sensor materials.

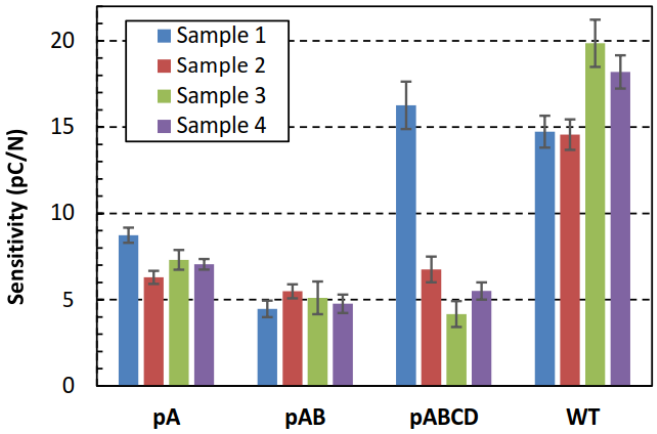

Figure 6. *Piezoelectric sensitivity of prepared BC films. Four sensors were constructed from each strain type films. The sensitivities were measured from five different excitation positions on either sides of the sensor. The plotted data represents averaged values and standard deviations (error bars) from total of ten excitations per sensor.*

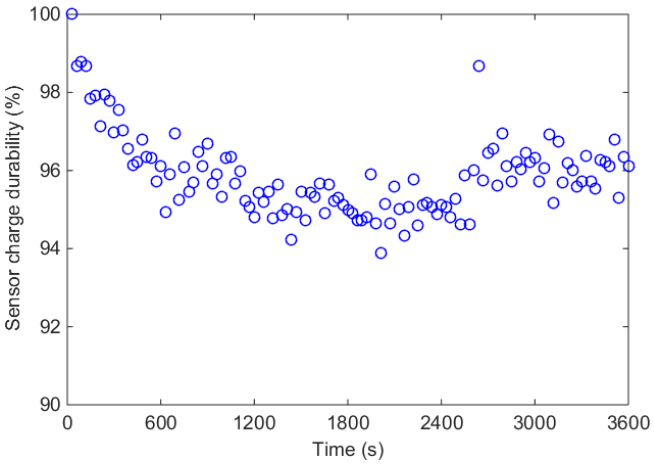

Figure 7*. The durability study of bacterial cellulose film sensor (produced by WT K. xylinus). The sensor's output charge is measured while exposed to sinusoidal (2 Hz) load cycles for 1 hour with a normal force of 1.4 N. The output values are presented as median amplitudes of 1 min data sections.*

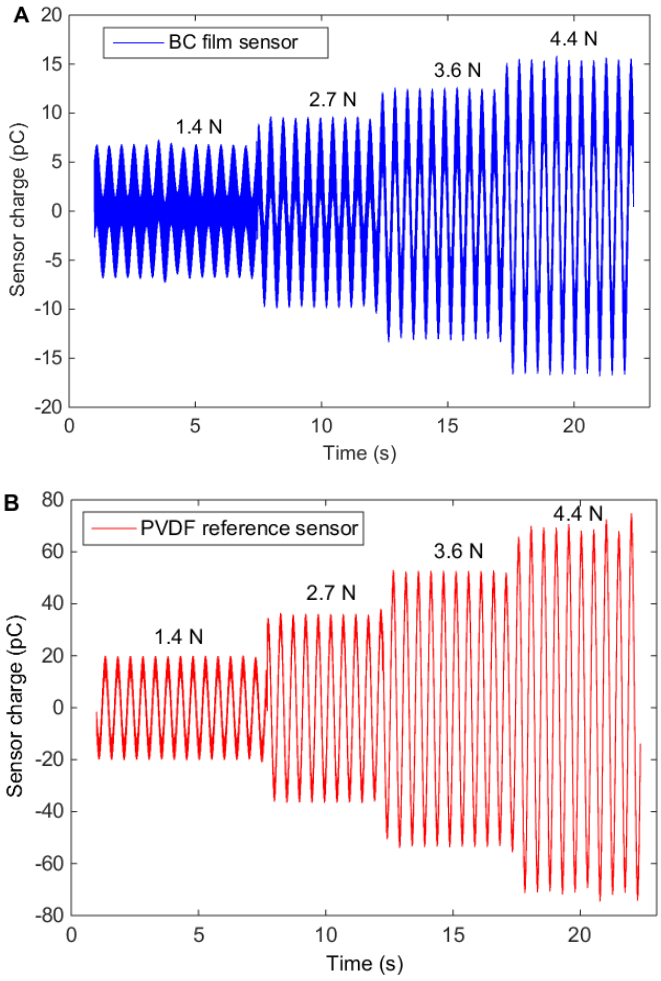

Figure 8*. Piezoelectric responses of (A) BC film (produced by WT K. xylinus) and (B) commercial PVDF (fabricated using sandwiched PET-Cu electrodes as contacts) sensors under increased mechanical load.*

To our knowledge, this is the first report to study and demonstrate piezoelectric sensitivities of BC films, restricting a direct comparison with existing literature. However, in comparison to piezoelectric sensitivities from wood cellulose and commercial piezoelectric materials (such as quartz and PVDF), a significant piezoelectric response was observed from BC films, indicating its potential application as sensor

material. From our previous study, we demonstrated piezoelectricity from wood-based cellulose nanofibril films (thickness 45µm) with d_{33} coefficients ranging from 5 to 7 pC/N [20,29,30]. Mahadeva et al. reported successful fabrication of hybrid paper from barium titanate nanoparticles and wood cellulose fiber, and demonstrated piezoelectric coefficient values (d_{33}, 4.8 pC/N) comparable with our study [28]. Subsequently, Mahadeva et al. reported remarkably higher piezoelectric coefficient (d_{33}, 45.7 pC/N) by incorporation of carboxymethylcellulose in the hybrid paper [27]. In the case of commercial materials, quartz has rather low but stable piezoelectricity (d_{33} coefficient ~2 pC/N) and among the poled polymers PVDF exhibits the highest piezoelectricity (d_{33} coefficient ~25 pC/N) [20,50]. Though the sensitivities obtained from this study align with previously reported in literature, variations exists between the tested BC film types.

In this proof-of-principle study, we have characterized the prepared BC films using stylus profilometer, SEM and XRD (CI of 88.6 to 97.5 %). The XRD spectra of the tested BC films observed from this study (2θ at 14.6^{o}, 16.9^{o} and 22.7^{o}) was similar to that reported for wood-based cellulose by Mahadeva et al. [reference Mahaveda 2014]. This similarity in the diffraction profile reflects the presence of native cellulose nanocrystals (cellulose I) in both bacterial [reference Feng-paper] and wood-based [reference Mahaveda 2014] celluloses and can reason for the piezoelectric responses from the BC film sensors. However, the alterations in the measured piezoelectric sensitivities for different BC film types cannot be understood solely based on the adopted characterization techniques. Differences in piezoelectric responses from BC film types with similar CI values (Table 1) indicate that the piezoelectric effects observed for the films depends more on the orientation of the bacterial cellulose crystal regions inside the films, rather than from the level of crystallinity. This is relied on a recent literature, where nanoscale investigations on cellulose nanocrystals reports evidences of a permanent dipole momentum resulting in piezoelectric responses [25].

It is to be noted that the BC films used in this study were not subjected to intentional polarization or orientation. Polarization of BC films is difficult due to its hygroscopic nature and strong entanglement

of cellulose fibers inside the film. Despite the expected random orientation of cellulose crystals inside the BC films, there may be some natural orientations taking place during the BC processing step. This type of non-intentional crystal orientation due to the fabrication process was also discussed in our previous report, wherein the piezoelectric properties of wood-based cellulose nanofibril films were studied [20].

However, since the BC films are naturally produced by *K. xylinus* cells grown under static conditions, possibilities of any growth related natural orientations to BC films cannot be ruled out. This type of growth related alterations to the piezoelectric crystal~~s~~ orientations may vary between the bacterial strains or cultivation conditions, which could explain the ~~alteration of~~ variations in piezoelectric sensitivities among the tested BC films. It is very challenging to characterize the crystalline orientations inside the BC films, and thus it is not included into the scope of this study. For further studies, one possibility could be to conduct a transmission electron microscope (TEM) analysis of microscopically thin slides cut from the BC films.

4. CONCLUSION

In summary, the work focused in investigating the applicability of BC films as a potential piezoelectric material. By transforming plasmids constructed via PCR-amplification and Gibson assembly, *K. xylinus* was engineered to harbor partial and complete bcs operon genes. The engineered *K. xylinus* strains overexpressing the bcs genes produced cellulose faster and with higher BC production titers, compared to the WT strain. As *K. xylinus* naturally produces BC from any carbon source, in large-scale production perspective, the genetic engineering costs become negligible which makes BC films several orders of magnitude cheaper than conventional piezoelectric materials. Mechanical and structural characterizations indicated alterations in film thickness and tensile stress 5 to 20 pC/N. This is the first study to demonstrate piezoelectric sensitivities of BC films, signifying its importance as a suitable sensor material complying with the principles of circular bioeconomy.

Supporting Information

Schematic representations of piezoelectric sensor assembly, setup and excitation positions; Photograph of tensile strength measurement system; Validation of *E. coli* transformants; Growth profiles of wild-type and engineered *K. xylinus* strains; Topography profile and thickness of BC films measured by stylus profilometer; stretching experiment curves of BC films measured using in-house built tensile measurement system and PCR primer sequence information.

AUTHOR INFORMATION

Corresponding Author

E.mail:- rahul.mangayil@tut.fi

Author Contributions

R.M., S.R., M.K., and S.T. designed the research; R.M. and J.L. engineered *K. xylinus* and conducted the biological study; A.P. characterized the BC films and assembled the piezoelectric sensor; S.R. conducted the piezoelectric sensitivity measurements; E.S. performed the SEM analysis of BC films; R.M., S.R., A.P., E.S., V.S., M.K. and S.T. analyzed the data; R.M, S.R., A.P. and S.T. wrote the paper; M.K. and S.T. supervised the work. All authors commented on the manuscript and has agreed to the final version.

Notes

The authors declare no competing financial interests.

ACKNOWLEDGEMENTS

We thank Mathias von Essen from the BioMediTech Institute and Faculty of Biomedical Sciences and Engineering at Tampere University of Technology for performing the BC film stretching measurements

and data analysis. We also thank Dr. Suvi Santala for proofreading the manuscript. R.M and V.S thanks Academy of Finland (Project no's. 272602 and 286450) for the financial support. MK acknowledges the sabbatical year financial support from The Finnish Cultural Foundation (Suomen Kulttuurirahasto).

REFERENCES

(1) Jozala, A. F.; de Lencastre-Novaes, L. C.; Lopes, A. M.; de Carvalho Santos-Ebinuma, V.; Mazzola, P. G.; Pessoa-Jr, A.; Grotto, D.; Gerenutti, M.; Chaud, M. V. Bacterial Nanocellulose Production and Application: A 10-Year Overview. *Appl. Microbiol. Biotechnol.* **2016**, *100* (5), 2063–2072.

(2) Lee, K. Y.; Buldum, G.; Mantalaris, A.; Bismarck, A. More than Meets the Eye in Bacterial Cellulose: Biosynthesis, Bioprocessing, and Applications in Advanced Fiber Composites. *Macromol. Biosci.* **2014**, *14* (1), 10–32.

(3) Hungund, B. S.; Gupta, S. G. Production of Bacterial Cellulose from Enterobacter Amnigenus GH-1 Isolated from Rotten Apple. *World J. Microbiol. Biotechnol.* **2010**, *26* (10), 1823–1828.

(4) Tanskul, S.; Amornthatree, K.; Jaturonlak, N. A New Cellulose-Producing Bacterium, *Rhodococcus* Sp. MI 2: Screening and Optimization of Culture Conditions. *Carbohydr. Polym.* **2013**, *92* (1), 421–428.

(5) Schramm, M.; Hestrin, S. Factors Affecting Production of Cellulose at the Air/ Liquid Interface of a Culture of *Acetobacter Xylinum*. *J. Gen. Microbiol.* **1954**, *11* (1), 123–129.

(6) Scott Williams, W. S.; Cannon, R. E. Alternative Environmental Roles for Cellulose Produced by *Acetobacter Xylinum*. *Appl. Environ. Microbiol.* **1989**, *55* (10), 2448–2452.

(7) Ross, P.; Mayer, R.; Benziman, M. Cellulose Biosynthesis and Function in Bacteria. *Microbiol. Rev.* **1991**, *55* (1), 35–58.

(8) Wu, R.-Q.; Li, Z.-X.; Yang, J.-P.; Xing, X.-H.; Shao, D.-Y.; Xing, K.-L. Mutagenesis Induced by High Hydrostatic Pressure Treatment: A Useful Method to Improve the Bacterial Cellulose Yield of a *Gluconoacetobacter Xylinus* Strain. *Cellulose* **2010**, *17* (2), 399–405.

(9) Hungund, B. S.; Gupta, S. G. Strain Improvement of *Gluconacetobacter Xylinus* NCIM 2526 for Bacterial Cellulose Production. *Afr. J. Biotechnol.* **2010**, *9* (32), 5170–5172.

(10) Bae, S. O.; Sugano, Y.; Ohi, K.; Shoda, M. Features of Bacterial Cellulose Synthesis in a Mutant Generated by Disruption of the Diguanylate Cyclase 1 Gene of *Acetobacter Xylinum* BPR 2001. *Appl. Microbiol. Biotechnol.* **2004**, *65* (3), 315–322.

(11) Kuo, C.-H.; Teng, H.-Y.; Lee, C.-K. Knock-out of Glucose Dehydrogenase Gene in *Gluconacetobacter Xylinus* for Bacterial Cellulose Production Enhancement. *Biotechnol. Bioprocess Eng.* **2015**, *20* (1), 18–25.

(12) Nakai, T.; Nishiyama, Y.; Kuga, S.; Sugano, Y.; Shoda, M. ORF2 Gene Involves in the Construction of High-Order Structure of Bacterial Cellulose. *Biochem. Biophys. Res. Commun.* **2002**, *295* (2), 458–462.

(13) Fu, L.; Zhang, J.; Yang, G. Present Status and Applications of Bacterial Cellulose-Based Materials for Skin Tissue Repair. *Carbohydr. Polym.* **2013**, *92* (2), 1432–1442.

(14) Wu, W.; Tassi, N. G.; Zhu, H.; Fang, Z.; Hu, L. Nanocellulose-Based Translucent Diffuser for Optoelectronic Device Applications with Dramatic Improvement of Light Coupling. *ACS Appl. Mater. Interfaces* **2015**, *7* (48), 26860–26864.

(15) Morales-Narváez, E.; Golmohammadi, H.; Naghdi, T.; Yousefi, H.; Kostiv, U.; Horák, D.; Pourreza, N.; Merkoçi, A. Nanopaper as an Optical Sensing Platform. *ACS Nano* **2015**, *9* (7), 7296–7305.

(16) Tuukkanen, S.; Julin, T.; Rantanen, V.; Zakrzewski, M.; Moilanen, P.; Lilja, K. E.; Rajala, S. Solution-

Processible Electrode Materials for a Heat-Sensitive Piezoelectric Thin-Film Sensor. *Synth. Met.* **2012**, *162* (21–22), 1987–1995.

(17) Porhonen, J.; Rajala, S.; Lehtimaki, S.; Tuukkanen, S. Flexible Piezoelectric Energy Harvesting Circuit with Printable Supercapacitor and Diodes. *IEEE Trans. Electron Devices* **2014**, *61* (9), 3303–3308.

(18) Vuorinen, T.; Zakrzewski, M.; Rajala, S.; Lupo, D.; Vanhala, J.; Palovuori, K.; Tuukkanen, S. Printable, Transparent, and Flexible Touch Panels Working in Sunlight and Moist Environments. *Adv. Funct. Mater.* **2014**, *24* (40), 6340–6347.

(19) Rajala, S.; Tuukkanen, S.; Halttunen, J. Characteristics of Piezoelectric Polymer Film Sensors with Solution-Processable Graphene-Based Electrode Materials. *IEEE Sens. J.* **2015**, *15* (6), 3102–3109.

(20) Rajala, S.; Siponkoski, T.; Sarlin, E.; Mettänen, M.; Vuoriluoto, M.; Pammo, A.; Juuti, J.; Rojas, O. J.; Franssila, S.; Tuukkanen, S. Cellulose Nanofibril Film as a Piezoelectric Sensor Material. *ACS Appl. Mater. Interfaces* **2016**, *8* (24), 15607–15614.

(21) Rajala, S. N. K.; Mettanen, M.; Tuukkanen, S. Structural and Electrical Characterization of Solution-Processed Electrodes for Piezoelectric Polymer Film Sensors. *IEEE Sens. J.* **2016**, *16* (6), 1692–1699.

(22) Rajala, S.; Lekkala, J. Film-Type Sensor Materials PVDF and EMFi in Measurement of Cardiorespiratory Signals a Review. *IEEE Sens. J.* **2012**, pp 439–446.

(23) Fukada, E. Piezoelectricity of Wood. *J. Phys. Soc. Jpn.* **1955**, *10* (2), 149–154.

(24) Fukada, E. Piezoelectricity as a Fundamental Property of Wood. *Wood. Sci. Technol.* **1968**, *2* (4), 299–307.

(25) Frka-Petesic, B.; Jean, B.; Heux, L. First Experimental Evidence of a Giant Permanent Electric-Dipole Moment in Cellulose Nanocrystals. *EPL.* **2014**, *107* (2), 28006.

(26) Csoka, L.; Hoeger, I. C.; Rojas, O. J.; Peszlen, I.; Pawlak, J. J.; Peralta, P. N. Piezoelectric Effect of

Cellulose Nanocrystals Thin Films. *ACS Macro Lett.* **2012**, *1* (7), 867–870.

(27) Mahadeva, S. K.; Walus, K.; Stoeber, B. Flexible and Robust Hybrid Paper with a Large Piezoelectric Coefficient. *J. Mater. Chem. C* **2016**, *4* (7), 1448–1453.

(28) Mahadeva, S. K.; Walus, K.; Stoeber, B. Piezoelectric Paper Fabricated via Nanostructured Barium Titanate Functionalization of Wood Cellulose Fibers. *ACS Appl. Mater. Interfaces* **2014**, *6* (10), 7547–7553.

(29) Rajala, S.; Vuoriluoto, M.; Rojas, O. J.; Franssila, S.; Tuukkanen, S. Piezoelectric Sensitivity Measurements of Cellulose Nanofibril Sensors. *XXI IMEKO 2015 World Congr. "Measurement Res. Ind. Conf. Proc.* **2015**, No. April 2016, 2–6.

(30) Tuukkanen, S.; Rajala, S. A Survey of Printable Piezoelectric Sensors. *SENSORS, 2015 IEEE*. **2015**, pp 1–4.

(31) Santala, S.; Efimova, E.; Koskinen, P.; Karp, M. T.; Santala, V. Rewiring the Wax Ester Production Pathway of *Acinetobacter Baylyi* ADP1. *ACS Synth. Biol.* **2014**, *3* (3), 145–151.

(32) Mangayil, R.; Santala, V.; Karp, M. Fermentative Hydrogen Production from Different Sugars by *Citrobacter* Sp. CMC-1 in Batch Culture. *Int. J. Hydrogen Energy* **2011**, *36* (23), 15187–15194.

(33) Park, S.; Baker, J. O.; Himmel, M. E.; Parilla, P. A.; Johnson, D. K. Cellulose Crystallinity Index: Measurement Techniques and Their Impact on Interpreting Cellulase Performance. *Biotechnol. Biofuels* **2010**, *3* (1), 10.

(34) Ramadan, K. S.; Sameoto, D.; Evoy, S. A Review of Piezoelectric Polymers as Functional Materials for Electromechanical Transducers. *Smart Mater. Struct.* **2014**, *23* (3), 33001.

(35) Krystynowicz, A.; Czaja, W.; Wiktorowska-Jezierska, A.; Gonçalves-Miśkiewicz, M.; Turkiewicz, M.; Bielecki, S. Factors Affecting the Yield and Properties of Bacterial Cellulose. *J. Ind. Microbiol.*

Biotechnol. **2002**, *29* (4), 189–195.

(36) Kuo, C.-H.; Chen, J.-H.; Liou, B.-K.; Lee, C.-K. Utilization of Acetate Buffer to Improve Bacterial Cellulose Production by *Gluconacetobacter Xylinus*. *Food Hydrocoll.* **2016**, *53*, 98–103.

(37) Naritomi, T.; Kouda, T.; Yano, H.; Yoshinaga, F. Effect of Lactate on Bacterial Cellulose Production from Fructose in Continuous Culture. *J. Ferment. Bioeng.* **1998**, *85* (1), 89–95.

(38) Brown Jr, R. M.; Saxena, I. M. Cellulose Biosynthesis: A Model for Understanding the Assembly of Biopolymers. *Plant Physiol. Biochem.* **2000**, *38* (1), 57–67.

(39) Shigematsu, T.; Takamine, K.; Kitazato, M.; Morita, T.; Naritomi, T.; Morimura, S.; Kida, K. Cellulose Production from Glucose Using a Glucose Dehydrogenase Gene (Gdh)-Deficient Mutant of *Gluconacetobacter Xylinus* and Its Use for Bioconversion of Sweet Potato Pulp. *J. Biosci. Bioeng.* **2005**, *99* (4), 415–422.

(40) Kawano, S.; Tajima, K.; Uemori, Y.; Yamashita, H.; Erata, T.; Munekata, M.; Takai, M. Cloning of Cellulose Synthesis Related Genes from *Acetobacter Xylinum* ATCC23769 and ATCC53582: Comparison of Cellulose Synthetic Ability between Strains. *DNA Res.* **2002**, *9* (5), 149–156.

(41) Tonouchi, N.; Tsuchida, T.; Yoshinaga, F.; Beppu, T.; Horinouchi, S. Characterization of the Biosynthetic Pathway of Cellulose from Glucose and Fructose in *Acetobacter Xylinum*. *Biosci. , Biotechnol. , and Biochem*. 1996, pp 1377–1379.

(42) Swissa, M.; Aloni, Y.; Weinhouse, H.; Benizman, M. Intermediary Steps in *Acetobacter Xylinum* Cellulose Synthesis: Studies with Whole Cells and Cell-Free Preparations of the Wild Type and a Celluloseless Mutant. *J. Bacteriol*. 1980, pp 1142–1150.

(43) Zhong, C.; Li, F.; Liu, M.; Yang, X. N.; Zhu, H. X.; Jia, Y. Y.; Jia, S. R.; Piergiovanni, L. Revealing Differences in Metabolic Flux Distributions between a Mutant Strain and Its Parent Strain

Gluconacetobacter Xylinus CGMCC 2955. *PLoS One* **2014**, *9* (6).

(44) Kornmann, H.; Duboc, P.; Marison, I.; Von Stockar, U. Influence of Nutritional Factors on the Nature, Yield, and Composition of Exopolysaccharides Produced by *Gluconacetobacter Xylinus* I-2281. *Appl. Environ. Microbiol.* **2003**, *69* (10), 6091–6098.

(45) Cavka, A.; Guo, X.; Tang, S.-J.; Winestrand, S.; Jönsson, L. J.; Hong, F. Production of Bacterial Cellulose and Enzyme from Waste Fiber Sludge. *Biotechnol. Biofuels* **2013**, *6* (1), 25.

(46) McKenna, B. A.; Mikkelsen, D.; Wehr, J. B.; Gidley, M. J.; Menzies, N. W. Mechanical and Structural Properties of Native and Alkali-Treated Bacterial Cellulose Produced by *Gluconacetobacter Xylinus* Strain ATCC 53524. *Cellulose* **2009**, *16* (6), 1047.

(47) Retegi, A.; Gabilondo, N.; Peña, C.; Zuluaga, R.; Castro, C.; Gañan, P.; de la Caba, K.; Mondragon, I. Bacterial Cellulose Films with Controlled Microstructure-Mechanical Property Relationships. *Cellulose* **2010**, *17* (3), 661–669.

(48) Jozala, A. F.; Pértile, R. A. N.; dos Santos, C. A.; de Carvalho Santos-Ebinuma, V.; Seckler, M. M.; Gama, F. M.; Pessoa, A. Bacterial Cellulose Production by *Gluconacetobacter Xylinus* by Employing Alternative Culture Media. *Appl. Microbiol. Biotechnol.* **2014**, *99* (3), 1181–1190.

(49) Segal, L.; Creely, J. J.; Martin, A. E.; Conrad, C. M. An Empirical Method for Estimating the Degree of Crystallinity of Native Cellulose Using the X-Ray Diffractometer. *Text. Res. J.* **1959**, *29* (10), 786–794.

(50) Regtien, P. P. L. *Sensors for Mechatronics*. Elsevier: Hengelo, The Netherlands, **2012**; Chapter 8, pp 219 - 221.

Table of Content Figure